

## Controlling the refractive index and third-order nonlinearity of polyimide/Ta<sub>2</sub>O<sub>5</sub> nanolaminates for optical applications

Elina Färm, Soroush Mehravar, Khanh Kieu, Nasser Peyghambarian, Mikko Ritala, Markku Leskelä, and Marianna Kemell

Citation: *Journal of Vacuum Science & Technology A* **37**, 060908 (2019); doi: 10.1116/1.5121589

View online: <https://doi.org/10.1116/1.5121589>

View Table of Contents: <https://avs.scitation.org/toc/jva/37/6>

Published by the [American Vacuum Society](#)

---

### ARTICLES YOU MAY BE INTERESTED IN

[Atomic layer deposition of silicon-based dielectrics for semiconductor manufacturing: Current status and future outlook](#)

*Journal of Vacuum Science & Technology A* **37**, 060904 (2019); <https://doi.org/10.1116/1.5113631>

[Photoassisted atomic layer deposition of oxides employing alkoxides as single-source precursors](#)

*Journal of Vacuum Science & Technology A* **37**, 060911 (2019); <https://doi.org/10.1116/1.5124100>

[Growth of cobalt films at room temperature using sequential exposures of cobalt tricarbonyl nitrosyl and low energy electrons](#)

*Journal of Vacuum Science & Technology A* **37**, 060906 (2019); <https://doi.org/10.1116/1.5113711>

[Reactivity in metal-Ge-Te systems: Thermodynamic predictions and experimental observations](#)

*Journal of Vacuum Science & Technology A* **37**, 061510 (2019); <https://doi.org/10.1116/1.5126109>

[Atomic layer deposition of h-BN\(0001\) multilayers on Ni\(111\) and chemical vapor deposition of graphene on h-BN\(0001\)/Ni\(111\)](#)

*Journal of Vacuum Science & Technology A* **37**, 060903 (2019); <https://doi.org/10.1116/1.5120628>

[Corrosion protection of Cu by atomic layer deposition](#)

*Journal of Vacuum Science & Technology A* **37**, 060902 (2019); <https://doi.org/10.1116/1.5116136>

---



**NEW**

# AVS Quantum Science

A new interdisciplinary home for impactful quantum science research and reviews

Co-Published by



**NOW ONLINE**

The banner features a dark blue background with a teal diagonal stripe in the top left corner containing the word 'NEW'. The main title 'AVS Quantum Science' is in large white font, with the subtitle 'A new interdisciplinary home for impactful quantum science research and reviews' below it. Logos for 'AIP Publishing' and 'AVS' are shown on the left. A teal button with 'NOW ONLINE' is at the bottom center. The background is decorated with various quantum science icons like atoms, molecules, and graphs.



# Controlling the refractive index and third-order nonlinearity of polyimide/Ta<sub>2</sub>O<sub>5</sub> nanolaminates for optical applications

Elina Färm,<sup>1,a)</sup> Soroush Mehravar,<sup>2</sup> Khanh Kieu,<sup>2</sup> Nasser Peyghambarian,<sup>2</sup> Mikko Ritala,<sup>1</sup> Markku Leskelä,<sup>1</sup> and Marianna Kemell<sup>1,b)</sup>

<sup>1</sup>Department of Chemistry, University of Helsinki, FI-00014 Helsinki, Finland

<sup>2</sup>College of Optical Sciences, University of Arizona, Tucson, Arizona 85721

(Received 26 July 2019; accepted 21 October 2019; published 11 November 2019)

In this study, the authors investigated third-order optical nonlinearity in polyimide/Ta<sub>2</sub>O<sub>5</sub> nanolaminates deposited by atomic layer deposition. Third harmonic signal measurements were done with a multiphoton microscope at an excitation wavelength of 1.55 μm, laser pulse duration of 150 fs, and estimated pulse energy of 1.2 nJ. Third-order optical nonlinearity is an essential property in optical signal applications for telecommunication. Transparency at telecommunication wavelengths and a high refractive index are desired for a material. Polyimide is optically transparent, enabling light guidance through the material. The refractive index of the material can be fine-tuned by combining polyimide with a substantially higher refractive index material—in this case, Ta<sub>2</sub>O<sub>5</sub>. The layer thicknesses in nanolaminates were varied, and the third harmonic generation was compared to plain polyimide and Ta<sub>2</sub>O<sub>5</sub> reference films. Third harmonic generation in the nanolaminates decreased slightly and refractive index increased with increasing Ta<sub>2</sub>O<sub>5</sub> content. Normalized third-order nonlinear susceptibilities,  $\chi^{(3)}$ , calculated for the nanolaminates were between the values of Ta<sub>2</sub>O<sub>5</sub> and polyimide and increased with increasing polyimide content. *Published by the AVS.* <https://doi.org/10.1116/1.5121589>

## I. INTRODUCTION

Polyimide is an optically transparent material, which makes it an interesting candidate for optical waveguide applications in telecommunication. In addition to optical transparency, also high third-order nonlinearity is needed for silicon nanophotonic devices.<sup>1–3</sup> Polyimides and polyisoimides with conjugated structures have also shown high third-order nonlinearities.<sup>4</sup> However, polyimide has a low refractive index (1.58 at 517 nm). Because third-order nonlinear susceptibility  $\chi^{(3)}$  increases with increasing refractive index,<sup>5,6</sup> the combination of polyimide with a higher refractive index material could result in even higher third-order nonlinearity. Among the various materials available for refractive index tuning,<sup>7</sup> Ta<sub>2</sub>O<sub>5</sub> is a well-known high refractive index material that exhibits also high third-order nonlinearity<sup>8,9</sup> and is transparent over a broad wavelength range of 300–8000 nm.<sup>10,11</sup> Moreover, Ta<sub>2</sub>O<sub>5</sub> is stable under laser radiation.<sup>12</sup>

Atomic layer deposition (ALD)<sup>13,14</sup> is an optimal technique to deposit thin films for optics because its unique self-limiting growth mechanism enables accurate thickness control and superior conformality also on large areas and patterned surfaces. The selection of materials available by ALD is wide, and also nanolaminates and other artificial structures can be formed in a well-controlled manner. The films are of high quality and pinhole-free.

Only few papers report third-order nonlinear properties of ALD-grown thin films. Five hundred nanometer thick ZnO/

Al<sub>2</sub>O<sub>3</sub> nanolaminates deposited by ALD showed enhanced third harmonic generation as compared to a plain ZnO film with a similar thickness.<sup>15,16</sup> TiO<sub>2</sub>/Al<sub>2</sub>O<sub>3</sub> nanolaminates<sup>16</sup> and ZnS/Al<sub>2</sub>O<sub>3</sub> mixture films<sup>17</sup> deposited by ALD showed third-order nonlinearities lower than plain TiO<sub>2</sub> and ZnS, respectively. In all these, a material with high third-order nonlinearity (ZnS, ZnO, or TiO<sub>2</sub>) was combined with Al<sub>2</sub>O<sub>3</sub> that does not exhibit high third-order nonlinearity.

We have earlier deposited polyimide/Ta<sub>2</sub>O<sub>5</sub> nanolaminates in a slot-waveguide ring resonator.<sup>18</sup> Our results showed confinement not only in the central air slot between two nanolaminate-coated rails, but also in the sub-10-nm vertical polyimide slots formed by the nanolaminate structure. Our devices showed high Q factors and low propagation losses, indicating their applicability in silicon nanophotonic devices.<sup>18</sup>

In this study, we investigated third-order nonlinearity of polyimide/Ta<sub>2</sub>O<sub>5</sub> nanolaminates deposited by atomic layer deposition. Both polyimide and Ta<sub>2</sub>O<sub>5</sub> have high third-order nonlinearities, which makes this system different to the nanolaminates studied earlier. The layer thicknesses in the nanolaminates were varied, and third harmonic generation in the nanolaminates was compared to plain polyimide and Ta<sub>2</sub>O<sub>5</sub> reference films.

## II. EXPERIMENT

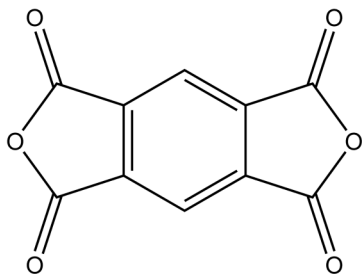
Polyimide/Ta<sub>2</sub>O<sub>5</sub> nanolaminates were deposited as in Ref. 19 in an F120 ALD reactor (ASM Microchemistry, Ltd.) on 5 × 5 cm<sup>2</sup> soda lime glass and Si substrates at 170 °C. The reactor was operated at a pressure of 10 mbar, and nitrogen was used as a carrier and purging gas. Precursors for the polyimide were PMDA (1,2,4,5-benzenetetracarboxylic anhydride, pyromellitic anhydride) and DAH (1,6-diaminohexane)<sup>20</sup>

Note: This paper is part of the 2020 Special Topic Collection on Atomic Layer Deposition (ALD).

<sup>a)</sup>Present address: ASM Microchemistry, Pietari Kalmin katu 3 F 2, FI-00560 Helsinki, Finland.

<sup>b)</sup>Electronic mail: marianna.kemell@helsinki.fi

PMDA  
= 1,2,4,5-Benzenetetracarboxylic anhydride  
= Pyromellitic dianhydride



DAH  
= 1,6-diaminohexane

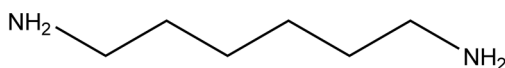


FIG. 1. Precursors used for polyimide films.

(Fig. 1) and for Ta<sub>2</sub>O<sub>5</sub> Ta(OEt)<sub>5</sub> and H<sub>2</sub>O.<sup>21</sup> PMDA, DAH, and Ta(OEt)<sub>5</sub> were vaporized at 150, 35, and 90 °C, respectively, from glass boats inside the reactor. H<sub>2</sub>O was vaporized from an external source at room temperature. Pulse durations were 4 s for PMDA, 3 s for DAH, 2 s for Ta(OEt)<sub>5</sub>, and 3 s for H<sub>2</sub>O. All purge durations were 5 s. The polyimide/Ta<sub>2</sub>O<sub>5</sub> nanolaminate films deposited using these processes are uniform.<sup>19</sup> The target structures of the nanolaminates are presented in Table I.

Thicknesses and refractive indices (at 517 nm) were determined by fitting transmission spectra with a program described in Ref. 22 where a one-term Sellmeier equation is used for refractive indices. The spectra were measured with a Hitachi U2000 spectrophotometer at the wavelength range of 370–1100 nm. The nanolaminates were modelled as single layers. A Hitachi S-4800 field emission scanning electron microscope was used for confirming the nanolaminate structures. Energy dispersive x-ray microanalysis (EDS) measurements were made with an Oxford INCA EDS spectrometer connected to the Hitachi SEM to estimate the actual amount of Ta<sub>2</sub>O<sub>5</sub> in the nanolaminates. The Ta<sub>2</sub>O<sub>5</sub> thicknesses

in the nanolaminates were calculated with a GMFILM program<sup>23</sup> from the *k* ratios measured at 25 keV for the Ta L $\alpha$  line. The plain Ta<sub>2</sub>O<sub>5</sub> film was used as the reference.

A multiphoton microscope described in Ref. 24 was used for measuring the third harmonic signal. The system has an erbium-doped mode-locked fiber laser as an excitation source. The laser operates at a wavelength of 1.55  $\mu$ m, and it is mode-locked by a carbon nanotube saturable absorber. The maximum average power of the laser was 60 mW with a repetition rate of 50 MHz, pulse duration of 150 fs, estimated pulse peak power of 8 kW, and pulse energy of 1.2 nJ.

### III. RESULTS AND DISCUSSION

#### A. Structure and refractive index

The nanolaminates consisted of six bilayers of polyimide + Ta<sub>2</sub>O<sub>5</sub> and were designed to have total thicknesses of 120 nm. The first layer of the bilayer was in most cases polyimide, followed by a Ta<sub>2</sub>O<sub>5</sub> film. The thicknesses of the polyimide and Ta<sub>2</sub>O<sub>5</sub> layers were varied to see the effect of the changing material content on the optical properties. For comparison, one nanolaminate was prepared with the reversed order of layers (first Ta<sub>2</sub>O<sub>5</sub>, then polyimide) and another one with 12 bilayers instead of six.

The target structures and their measured thicknesses, refractive indices, and Ta<sub>2</sub>O<sub>5</sub> thicknesses are shown in Table I. It has been observed earlier that the actual layer thicknesses in nanolaminates may differ from the target values.<sup>18,19</sup> Therefore, the refractive indices and nonlinear optical properties are reported here as a function of the measured Ta<sub>2</sub>O<sub>5</sub> thickness in each nanolaminate. The lowest refractive index (1.58 at 517 nm) was measured for the polyimide reference film and the highest refractive index (2.10 at 517 nm) for the Ta<sub>2</sub>O<sub>5</sub> film. As expected, the refractive indices of the nanolaminates increased with increasing Ta<sub>2</sub>O<sub>5</sub> content. This is also seen in Fig. 2. From Fig. 2, it is also clear that the refractive index does not show a perfect linear dependence on the measured Ta<sub>2</sub>O<sub>5</sub> content. Instead, the nanolaminates have lower than expected refractive indices. This is probably due to inaccuracy in the Ta<sub>2</sub>O<sub>5</sub> thickness measurement by EDS. The relative error is estimated to be about  $\pm 10\%$ . The UV-vis transmission measurement allows a highly accurate determination of refractive index and film thickness for a single uniform layer of a homogeneous material. The simplifying one-layer model employed here probably introduces some

TABLE I. Target structures and measured properties of polyimide/Ta<sub>2</sub>O<sub>5</sub> nanolaminates.

Target structure	Nominal Ta <sub>2</sub> O <sub>5</sub> content (vol. %)	Thickness (nm)	<i>n</i> (517 nm)	Measured Ta <sub>2</sub> O <sub>5</sub> thickness (nm)
Polyimide reference	0	121	1.58	0
6 × (15 nm polyimide + 5 nm Ta <sub>2</sub> O <sub>5</sub> )	25	116	1.66	25
6 × (10 nm polyimide + 10 nm Ta <sub>2</sub> O <sub>5</sub> )	50	120	1.81	62
6 × (5 nm polyimide + 15 nm Ta <sub>2</sub> O <sub>5</sub> )	75	122	1.83	81
Ta <sub>2</sub> O <sub>5</sub> reference	100	120	2.10	120
6 × (10 nm Ta <sub>2</sub> O <sub>5</sub> + 10 nm polyimide)	50	122	1.73	52
12 × (10 nm polyimide + 10 nm Ta <sub>2</sub> O <sub>5</sub> )	50	218	1.91	–

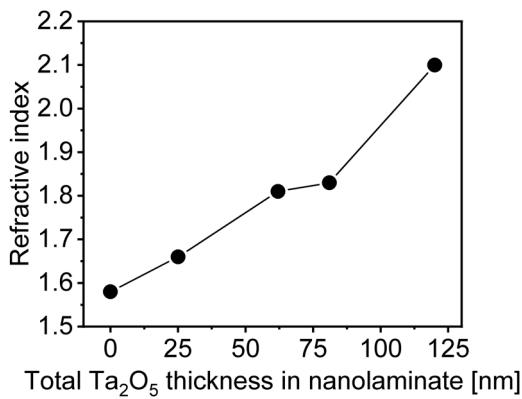


FIG. 2. Refractive indices of the nanolaminates and polyimide and Ta<sub>2</sub>O<sub>5</sub> reference samples at 517 nm as a function of measured Ta<sub>2</sub>O<sub>5</sub> thickness.

error both to the total film thickness and to the refractive index. Despite this, the refractive index dependence is nearly linear over the nominal composition range from 0 to 50 vol. % Ta<sub>2</sub>O<sub>5</sub> (measured Ta<sub>2</sub>O<sub>5</sub> thickness of 0–62 nm), indicating that the refractive index can be tuned in a straightforward manner over this range.

Figure 3 shows a nanolaminate structure with 12 bilayers and confirms clearly that the structure indeed consists of distinct polyimide and Ta<sub>2</sub>O<sub>5</sub> layers.

### B. Third-order nonlinearity

Third-order nonlinearities of the polyimide/Ta<sub>2</sub>O<sub>5</sub> nanolaminates were studied with a multiphoton microscope.<sup>24</sup> The measurements were made similarly as in Refs. 15 and 16. The laser spot diameter was about 1.8 μm. The third harmonic generation (THG) signal was selected using a 520 ± 10 nm band-pass filter. For each sample, three (3) areas about 1 mm apart from each other were measured. The THG signal was averaged over 512 × 512 points on each rectangular 260 × 260 μm<sup>2</sup> measurement area.

All the polyimide/Ta<sub>2</sub>O<sub>5</sub> nanolaminates as well as plain polyimide and Ta<sub>2</sub>O<sub>5</sub> films produced a third harmonic signal. The measured third harmonic signals are shown in Fig. 4. No second harmonic generation was detected. The highest third harmonic generation was measured for the polyimide reference film and the lowest for the Ta<sub>2</sub>O<sub>5</sub> reference film.

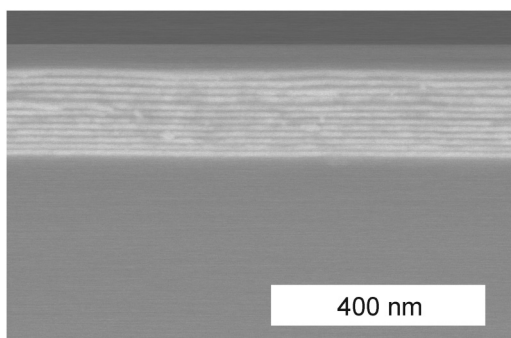


FIG. 3. SEM image of a polyimide/Ta<sub>2</sub>O<sub>5</sub> nanolaminate with 12 bilayers. Dark layers = polyimide, bright layers = Ta<sub>2</sub>O<sub>5</sub>.

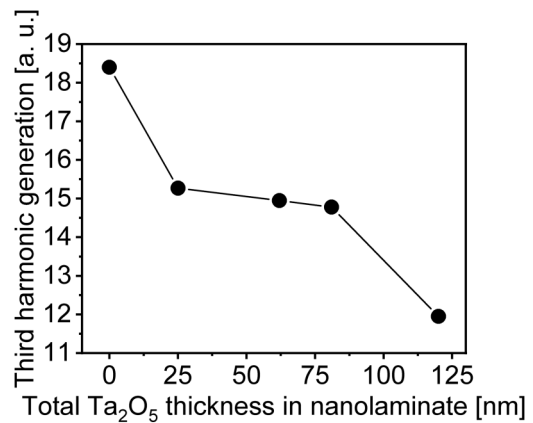


FIG. 4. Third harmonic generation in polyimide/Ta<sub>2</sub>O<sub>5</sub> nanolaminates and polyimide and Ta<sub>2</sub>O<sub>5</sub> reference samples as a function of measured Ta<sub>2</sub>O<sub>5</sub> thickness.

Among the nanolaminates, the one with nominally 75 vol. % Ta<sub>2</sub>O<sub>5</sub> (81 nm Ta<sub>2</sub>O<sub>5</sub>) gave the lowest third harmonic signal, and the third harmonic generation seemed to increase slightly with increasing polyimide content. However, the third harmonic values were very close to each other, and the differences between the different nanolaminates may not be significant. Despite that, the various nanolaminates have clearly different refractive indices as shown above in Table I and Fig. 2. Thus, the addition of Ta<sub>2</sub>O<sub>5</sub> in the nanolaminate increases the refractive index while still maintaining the THG at almost constant level, which allows to tune the refractive index and THG independently and, thus, makes these nanolaminates attractive to use in silicon nanophotonics. The samples with 50–75 vol. % (or 62–81 nm) Ta<sub>2</sub>O<sub>5</sub> seem to be the optimum because they combine a high THG and a high refractive index.

Normalized third-order nonlinear susceptibilities,  $\chi^{(3)}$ , were calculated from the THG values as in Refs. 15 and 16. Briefly, the THG signal is proportional to the square of  $(V \cdot \chi^{(3)})$ .<sup>15,16</sup> Taking into account that the illuminated area is equal for all samples,  $\chi^{(3)}$  can be calculated if the film thickness is known. Before calculating  $\chi^{(3)}$ , the measured THG signals were first normalized to the THG signal measured for the plain polyimide film, and the film thicknesses were normalized to the thickness of the plain polyimide film. The relative error is estimated to be below 10%. The results are shown in Table II and Fig. 5.

The relative  $\chi^{(3)}$  values of the plain polyimide and Ta<sub>2</sub>O<sub>5</sub> were quite close to each other. This is in agreement with the literature. The  $\chi^{(3)}$  value for PMDA-DAH has not been reported in the literature, but for PMDA-PDA (PDA = *p*-phenylenediamine),  $\chi^{(3)}$  of  $7 \times 10^{-13}$  esu at the fundamental wavelength of 1907 nm has been reported.<sup>4</sup> The  $\chi^{(3)}$  reported for Ta<sub>2</sub>O<sub>5</sub> is  $2 \times 10^{-13}$  esu at 1550 nm.<sup>9</sup> All the nanolaminate films had lower third-order nonlinear susceptibilities than the plain polyimide. The relative  $\chi^{(3)}$  values were so close to each other that the differences between different samples are probably not significant; in addition, there is no enhancement in  $\chi^{(3)}$  by the

TABLE II. Measured and normalized THG and normalized third-order nonlinear susceptibility for polyimide (PI) Ta<sub>2</sub>O<sub>5</sub>, and nanolaminates.

Sample	Measured Ta <sub>2</sub> O <sub>5</sub> thickness (nm)	Measured THG	THG normalized to PI	$\chi^{(3)}$ normalized
Polyimide	0	18.44	1.00	1.00
6 × (15 nm polyimide + 5 nm Ta <sub>2</sub> O <sub>5</sub> )	25	15.27	0.83	0.95
6 × (10 nm polyimide + 10 nm Ta <sub>2</sub> O <sub>5</sub> )	62	14.95	0.81	0.91
6 × (5 nm polyimide + 15 nm Ta <sub>2</sub> O <sub>5</sub> )	81	14.78	0.80	0.89
Ta <sub>2</sub> O <sub>5</sub>	120	11.95	0.65	0.81
6 × (10 nm Ta <sub>2</sub> O <sub>5</sub> + 10 nm polyimide)	52	14.44	0.78	0.88
12 × (10 nm polyimide + 10 nm Ta <sub>2</sub> O <sub>5</sub> )	–	13.24	0.72	0.47

nanolaminate structure. In that sense, our results are in agreement with those reported for TiO<sub>2</sub>/Al<sub>2</sub>O<sub>3</sub> nanolaminates<sup>16</sup> and with our earlier observations of ZnS/Al<sub>2</sub>O<sub>3</sub> mixture films<sup>17</sup> but different from what was observed for ZnO/Al<sub>2</sub>O<sub>3</sub> nanolaminates.<sup>15,16</sup>

We studied also the effect of film thickness on the third harmonic generation. Interestingly, film thickness—at least over the range of our samples—did not seem to affect the third harmonic generation significantly. In the case of polyimide, the third harmonic signals measured for 121 and 189 nm thick films were very close to each other. The same was true for Ta<sub>2</sub>O<sub>5</sub> films when the film thickness was increased by 50 nm. The same effect was seen in the polyimide/Ta<sub>2</sub>O<sub>5</sub> nanolaminates, too: doubling the nanolaminate target thickness to 240 nm while keeping the thicknesses of polyimide and Ta<sub>2</sub>O<sub>5</sub> layers at 10 nm did not increase the third harmonic generation. The THG signal is enhanced by interfaces,<sup>25,26</sup> and thus, doubling the number of layers should result in a higher signal. However, in the case of our polyimide/Ta<sub>2</sub>O<sub>5</sub> nanolaminates, this was obviously not the case.

The harmonic signal varies sinusoidally with film thickness, showing maxima at thicknesses corresponding to the coherence length and its odd multiples and minima at thicknesses corresponding to its even multiples. Das *et al.*<sup>27</sup> studied THG in sputtered TiO<sub>2</sub> thin films as a function of thickness. The optimum (highest) THG was found in 180 nm

thick films, in agreement with the calculated coherence length of 190 nm at the fundamental wavelength of 800 nm.<sup>27</sup> In our case, it is obvious that the thicknesses of all films are far below the coherence length. Therefore, we expect slow variation in the THG signal with the film thicknesses in our experiments. To confirm this, the coherence lengths  $L_c$  were calculated from the following equation:

$$L_c = \frac{\lambda}{6(n_{517} - n_{1550})}, \quad (1)$$

where  $\lambda$  is the excitation wavelength and  $n_{517}$  and  $n_{1550}$  are the refractive indices at the excitation wavelength (1550 nm) and at the THG wavelength (517 nm), respectively.

The refractive indices for Ta<sub>2</sub>O<sub>5</sub> and PMDA-DAH films at 1550 nm were extrapolated from the UV-vis data<sup>22</sup> and were 2.01 and 1.46, respectively. Thus, the coherence lengths at 1550 nm were 2.9  $\mu$ m for Ta<sub>2</sub>O<sub>5</sub> and 2.2  $\mu$ m for polyimide.

In contrast to the behavior observed in Ta<sub>2</sub>O<sub>5</sub>, polyimide, and their nanolaminates, ALD-grown Nb<sub>2</sub>O<sub>5</sub> thin films measured for comparison showed increasing third harmonic signal with increasing film thickness (see Fig. 6). The Nb<sub>2</sub>O<sub>5</sub> films were deposited at 200–230 °C from Nb(OEt)<sub>5</sub> and H<sub>2</sub>O,<sup>28</sup> and their thicknesses were between 112 and 288 nm. Thus, the dependence of THG intensity on film thickness seems to be different for different thin film materials. The coherence length for Nb<sub>2</sub>O<sub>5</sub> was estimated to be the same order of magnitude as for Ta<sub>2</sub>O<sub>5</sub> and polyimide.

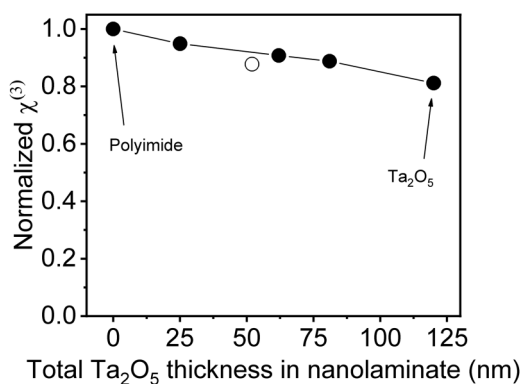


FIG. 5. Normalized third-order nonlinear susceptibility,  $\chi^{(3)}$ , as a function of measured Ta<sub>2</sub>O<sub>5</sub> thickness. Closed circles = nanolaminates with polyimide as the first layer. Open circle = the nanolaminate with Ta<sub>2</sub>O<sub>5</sub> as the first layer.

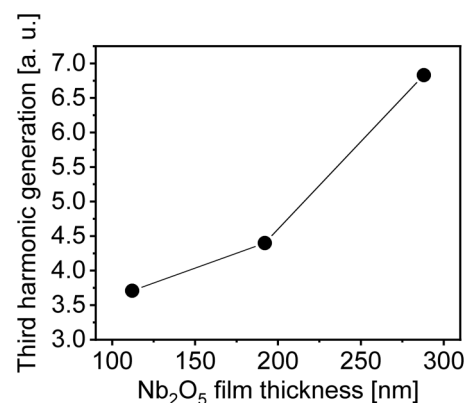


FIG. 6. THG measured for ALD-Nb<sub>2</sub>O<sub>5</sub> films as a function of film thickness.

#### IV. SUMMARY AND CONCLUSIONS

Third-order optical nonlinearity in ALD-grown polyimide/Ta<sub>2</sub>O<sub>5</sub> nanolaminates was studied by measuring third harmonic generation with a multiphoton microscope. Various nanolaminates with different layer thicknesses were studied, and their third harmonic signals and refractive indices were compared to those measured of polyimide and Ta<sub>2</sub>O<sub>5</sub> reference films. Both polyimide and Ta<sub>2</sub>O<sub>5</sub> showed third harmonic generation. Third harmonic generation in the nanolaminates decreased very slightly, and the refractive index increased with increasing Ta<sub>2</sub>O<sub>5</sub> content. This makes it possible to fine-tune the refractive index while keeping the third harmonic signal almost constant. Normalized third-order nonlinear susceptibilities,  $\chi^{(3)}$ , calculated for the nanolaminates were between the values of Ta<sub>2</sub>O<sub>5</sub> and polyimide and increased almost linearly with increasing polyimide content.

#### ACKNOWLEDGMENTS

The authors thank Lasse Karvonen and Antti Säynätjoki for sharing their insight into measuring thin films with multiphoton microscopy and for discussion on the results. The work of the Helsinki group was funded partly by the Academy of Finland (Grant No. 251142) and the Finnish Centre of Excellence in Atomic Layer Deposition. The Arizona group acknowledges support from TRIF Photonics at University of Arizona and NSF CIAN ERC.

<sup>1</sup>M. Borghi, C. Castellani, S. Signorini, A. Trenti, and L. Pavesi, *J. Opt.* **19**, 093002 (2017).

<sup>2</sup>S. Fathpour, *Nanophotonics* **4**, 143 (2015).

<sup>3</sup>C. Koos *et al.*, *Nat. Photonics* **3**, 216 (2009).

<sup>4</sup>S. Morino, T. Yamashita, K. Horie, T. Wada, and H. Sasabe, *React. Funct. Polym.* **44**, 183 (2000).

<sup>5</sup>H. Tichá and L. Tichý, *J. Optoelectron. Adv. Mater.* **4**, 381 (2002).

<sup>6</sup>M. Arif, M. Shkir, S. AlFaify, A. Sanger, P. M. Vilarinho, and A. Singh, *Opt. Laser Technol.* **112**, 539 (2019).

<sup>7</sup>J. Loste, J.-M. Lopez-Cuesta, L. Billon, H. Garay, and M. Save, *Prog. Polym. Sci.* **89**, 133 (2019).

<sup>8</sup>C.-Y. Tai, J. Wilkinson, N. Perney, M. Netti, F. Cattaneo, C. Finlayson, and J. Baumberg, *Opt. Express* **12**, 5110 (2004).

<sup>9</sup>R. Y. Chen, M. D. B. Charlton, and P. G. Lagoudakis, *Opt. Lett.* **34**, 1135 (2009).

<sup>10</sup>A. Z. Subramanian, G. S. Murugan, M. N. Zervas, and J. S. Wilkinson, *Opt. Commun.* **285**, 124 (2012).

<sup>11</sup>M. Belt, M. L. Davenport, J. E. Bowers, and D. J. Blumenthal, *Optica* **4**, 532 (2017).

<sup>12</sup>J. Jasapara, A. V. V. Nampoothiri, W. Rudolph, D. Ristau, and K. Starke, *Phys. Rev. B* **63**, 045117 (2001).

<sup>13</sup>V. Miikkulainen, M. Leskelä, M. Ritala, and R. L. Puurunen, *J. Appl. Phys.* **113**, 021301 (2013).

<sup>14</sup>A. J. M. Mackus, J. R. Schneider, C. MacIsaac, J. G. Baker, and S. F. Bent, *Chem. Mater.* **31**, 1142 (2019).

<sup>15</sup>L. Karvonen *et al.*, *Appl. Phys. Lett.* **103**, 031903 (2013).

<sup>16</sup>L. Karvonen *et al.*, *Proc. SPIE* **8982**, 898200 (2014).

<sup>17</sup>E. Färm *et al.*, "Tuning the optical properties of ZnS/Al<sub>2</sub>O<sub>3</sub> thin films for nonlinear optics" (unpublished).

<sup>18</sup>A. Autere *et al.*, *Opt. Express* **23**, 26940 (2015).

<sup>19</sup>L. D. Salmi, E. Puukilainen, M. Vehkamäki, M. Heikkilä, and M. Ritala, *Chem. Vapor Depos.* **15**, 221 (2009).

<sup>20</sup>M. Putkonen, J. Harjuoja, T. Sajavaara, and L. Niinistö, *J. Mater. Chem.* **17**, 664 (2007).

<sup>21</sup>K. Kukli, M. Ritala, and M. Leskelä, *J. Electrochem. Soc.* **142**, 1670 (1995).

<sup>22</sup>M. Ylilammi and T. Ranta-aho, *Thin Solid Films* **232**, 56 (1993).

<sup>23</sup>R. A. Waldo, *Microbeam Anal.* **1988**, 310 (1988).

<sup>24</sup>K. Kieu, S. Mehravar, R. Gowda, R. A. Norwood, and N. Peyghambarian, *Biomed. Opt. Express* **4**, 2187 (2013).

<sup>25</sup>T. Y. F. Tsang, *Phys. Rev. A* **52**, 4116 (1995).

<sup>26</sup>Y. Barad, H. Eisenberg, M. Horowitz, and Y. Silberberg, *Appl. Phys. Lett.* **70**, 922 (1997).

<sup>27</sup>S. Kumar Das, C. Schwanke, A. Pfuch, W. Seeber, M. Bock, G. Steinmeyer, T. Elsaesser, and R. Grunwald, *Opt. Express* **19**, 16985 (2011).

<sup>28</sup>K. Kukli, M. Ritala, M. Leskelä, and R. Lappalainen, *Chem. Vapor Depos.* **4**, 29 (1998).